PCCP

PAPER

Cite this: *Phys. Chem. Chem. Phys.*, 2016, **18**, 25756

Infrared spectra and band strengths of CH_3SH, an interstellar molecule

R. L. Hudson

Received 2nd March 2016,
Accepted 28th August 2016

DOI: 10.1039/c6cp01475e

www.rsc.org/pccp

Three solid phases of CH_3SH (methanethiol or methyl mercaptan) have been prepared and their mid-infrared spectra recorded at 10–110 K, with an emphasis on the 17–100 K region. Refractive indices have been measured at two temperatures and used to estimate ice densities and infrared band strengths. Vapor pressures for the two crystalline phases of CH_3SH at 110 K are estimated. The behavior of amorphous CH_3SH on warming is presented and discussed in terms of Ostwald's step rule. Comparisons to CH_3OH under similar conditions are made, and some inconsistencies and ambiguities in the CH_3SH literature are examined and corrected.

1. Introduction

Measurements of the infrared (IR) spectra of interstellar and solar-system molecules remain both a challenge for astrochemists and a need for astronomical observers. Many such molecules are relatively stable and carry little health or safety hazards (*e.g.*, H_2O, CO_2), while others are more difficult to study for various reasons (*e.g.*, HCN, HNC, HNCNH). Into this latter category we place CH_3SH, known as methanethiol or methylmercaptan, a compound that was first detected in the interstellar medium (ISM) in 1979,[1] but which has received little attention from laboratory astrochemists. This molecule is one of many for which an interstellar synthesis on a cold icy grain might be expected followed by ejection into the gas-phase ISM, and so studies of the properties of solid-phase CH_3SH are of interest. Aside from interstellar environments, CH_3SH is also suspected to be an atmospheric component of Jupiter and other gas giants. The relevance of CH_3SH to astrobiology and pre-biological chemistry has been explored, and CH_3SH has been considered as a possible biomarker for Mars and other worlds.[2–4]

From purely a molecular vantage point, CH_3SH would appear to be a good candidate for comparison studies to its lighter relation, CH_3OH. However, although the study of two crystalline phases of CH_3OH has a long history,[5–8] a literature search reveals little comparable activity for the solid phases of CH_3SH. One can speculate that this lack of work on CH_3SH is related to the compound's notorious odor, much higher cost, and lower recommended health and safety exposure levels as compared to CH_3OH.

The relevant literature reports that there are two crystalline phases of CH_3SH at low pressure or vacuum conditions, that 137.6 K is the transition temperature between them, and that the conversion from one phase to the other is quite slow.[5] Rapid cooling of liquid CH_3SH to its freezing point, 150.2 K, produces the high-temperature crystalline structure, which we designate as the β phase. Continued rapid cooling locks in this phase to the extent that it can be studied well below the solid–solid transition temperature. In contrast, holding the β phase just below 137.6 K for several hours, and then slowly cooling it further, produces the low-temperature crystalline solid, the α phase. The two crystalline phases of CH_3CN, acetonitrile, show a similar behavior and give rise to two distinct types of radiation-produced free-radicals.[9,10]

The only detailed IR spectroscopic studies of solid CH_3SH available are from May and Pace[11,12] and Wolff and Szydlowski,[13] all with grating spectrometers of unspecified resolution. Unfortunately, each paper lacks important details about sample preparation and appears to be limited to a single ice temperature ($\sim$77 K). Also, none of those three papers included both (a) specific values for the thicknesses of the crystalline samples whose IR spectra were shown and (b) a numerical scale on the vertical axis, making absolute intensity determinations impossible. Most confusing of all is that there is an internal inconsistency among the text, figures, and table of May and Pace,[12] so that their results disagree with their earlier work[11] and that of Wolff and Szydlowski.[13] A one-sentence footnote near the end of the latter paper noted that a problem existed, but gave no unequivocal solution.

Over the past 30 years our group has made multiple excursions into the spectroscopy and chemistry of icy solids containing various sulfur-bearing molecules and ions. Our early work explored S_2 in cometary ices,[14] later studies investigated the radiation chemistry of $H_2O + H_2S$ and $H_2O + SO_2$ ice mixtures for application to the Galilean satellites,[15] and subsequent experiments covered sulfur oxyanions, H_2SO_4, and two hydrates

Astrochemistry Laboratory, NASA Goddard Space Flight Center, Greenbelt, MD 20771, USA. E-mail: reggie.hudson@nasa.gov

of sulfuric acid.[16,17] Most recently we have examined the connection between NH_4SH and Jupiter's Great Red Spot.[18,19]

We now turn from these inorganic sulfur species to the organosulfur compound CH_3SH, addressing difficulties and inconsistencies in some earlier publications on this molecule. We present the first mid-IR spectra of the amorphous phase of CH_3SH alongside new infrared spectra for two crystalline phases of this compound. Methods for the preparation of each phase are described and the thermal behavior of each phase is explored. We report the first refractive indices of solid CH_3SH, and use them to calculate the densities of the compound's solid phases and also, for the first time, IR band strengths. An estimate of CH_3SH vapor pressures at 110 K is made for the two crystalline phases examined. We also briefly compare the thermal behaviors and spectra of solid CH_3SH and solid CH_3OH. Our experience suggests that only with such laboratory work to measure spectra and other properties of ices can their astrochemical importance be explored with confidence.

2. Experimental

The equipment used was similar, and in most cases identical, to that employed in our recent papers on reference IR spectra and optical constants.[20] Methanethiol gas was deposited onto a pre-cooled KBr substrate held at 10–110 K inside a vacuum chamber ($\sim 10^{-8}$ torr). A shower-head type nebulizer, placed a few centimeters from the substrate and perpendicular to it, ensured a uniform ice deposition. Sample thicknesses varied from about 0.5 to 12 μm. The cryostat used for most of the experiments was a model DE-202AI from ARS (Macungie, Pennsylvania, USA) with a minimum temperature that was usually between 15 and 17 K, which for convenience we refer to simply as 17 K. Sigma Aldrich was the source of all reagents used, with all purities being above 99.5%.

Thicknesses and refractive indices of CH_3SH ices were measured with a double-laser interferometer system[21] using two lasers with $\lambda = 670$ nm at angles of 8.242° and 45.00° from a perpendicular to the substrate's surface. The lasers' light that reflected from the substrate and the ice sample was detected with a photodiode and with a Thorlabs detector and then collected and stored with WaveScan 2.0 software. The periods of the resulting fringe patterns were obtained by fitting the signal *vs.* time data using a procedure similar to that of Romanescu *et al.*,[22] and incorporated into a computer routine with Microsoft Excel's Solver add-in.

Most infrared spectra of CH_3SH ices were recorded with a Mattson Polaris FTIR instrument over 4000–600 cm^{-1} at a resolution of 1 cm^{-1} with 100 accumulations per spectrum. In a few cases, spectra were acquired with a Thermo iS50 IR spectrometer using similar settings.

As in our recent papers on CO_2 and hydrocarbons, the key to preparing the desired solid phase of CH_3SH was not necessarily the vacuum system's base pressure, the cryostat's lowest temperature, or the sample's thickness. The single most important parameter was the rate of deposition. The rates of deposition used for the present work gave increases in the resulting ice's thickness of 1–15 μm $hour^{-1}$.

Concerning hazards encountered, we repeat the observation that CH_3SH "is a flammable, moderately toxic gas characterized by an obnoxious, evil stench."[23] Sun *et al.* recently concluded that CH_3SH has one of the lowest odor thresholds and highest volatilities of any volatile organic sulfur compound.[24]

3. Results

3.1 Refractive indices

The left-hand side of Fig. 1 shows a typical set of interference fringes recorded during the growth of a CH_3SH ice. The periods t_1 and t_2 of the two fringe patterns, from our laser angles of θ_1 = 8.242° (lower trace) and θ_2 = 45.00° (upper trace), were combined with eqn (1) to calculate n for the sample.

$$n = \sqrt{\frac{\sin^2\theta_2 - (t_1/t_2)^2\sin^2\theta_1}{1-(t_1/t_2)^2}} \quad (1)$$

Few, if any, graphical comparisons of n values measured for icy solids in different laboratories have been published, and so in the right-hand panel of Fig. 1 we compare some of our own results to those in the literature. We performed at least three measurements in each case, and at the published temperature

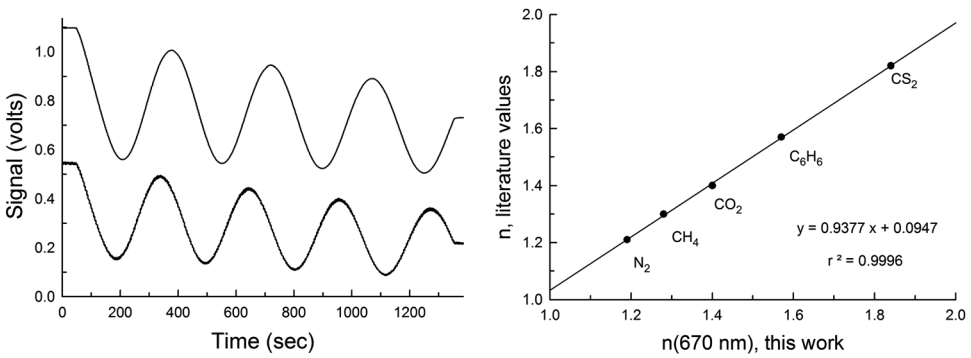

Fig. 1 Left: Interference fringes recorded during the growth of crystalline CH_3SH at 100 K. The horizontal line at the beginning and end of each fringe pattern indicates where the CH_3SH flow was started and stopped, respectively. Right: Values of n(670 nm) measured for five ices compared to literature values for the same.

for the reference material. Although our preference was to compare only with values of n that were accompanied by IR spectra, to ensure that the same ice phases were being studied, most of the relevant publications report either n or IR spectra, but not both. Three exceptions are work from over 50 years ago by Yamada and Person on crystalline CS_2, CO_2, and C_6H_6.[25–27] Those authors' results are included in Fig. 1, to which we have added points for CH_4 and N_2 from Satorre *et al.*,[28] each solid almost certainly being crystalline. The agreement in Fig. 1 is not perfect, but certainly is acceptable given differences in experimental conditions (*e.g.*, wavelength), and argues for the reliability of our measurements. Additional comparison studies are in progress.

Triplicate measurements with CH_3SH, using the procedure already described, gave n(17 K) = 1.417 for amorphous CH_3SH and n(100 K) = 1.542 for crystalline CH_3SH, with uncertainties (standard errors) of about ±0.005 based on a propagation-of-error treatment.[29] These n_{CH_3SH} values were used with eqn (2) to measure the thickness (h) of each ice sample studied. In this equation, N_{fr} is the number of interference fringes recorded during an ice's growth.[30]

$$h = \frac{N_{fr}\lambda}{2\sqrt{n^2 - \sin^2\theta}} \quad (2)$$

We should add that n(100 K) = 1.542 was used for all crystalline CH_3SH ices from 17 to 110 K as experience has shown us that n varies little over such a temperature range, provided that the ice's phase does not change. A few checks of n_{CH_3SH} at other temperatures gave results in agreement with this assumption. A similar assumption was made regarding the densities of α and β crystalline CH_3SH ices, which finds support in the similarities of the densities of the α and β forms of CH_3OH.[7,8,31]

3.2 Infrared spectra

Three forms of solid CH_3SH were studied in this work, one amorphous form and two crystalline phases, with amorphous CH_3SH being the easiest to prepare. Depositions of gas-phase CH_3SH onto a substrate at 15–30 K always resulted in an amorphous ice, this phase being identified by rounded IR peaks with little or no spectral sub-structure and an overall resemblance to the spectrum of liquid CH_3SH.[11] The literature methods for making the α (low-temperature) and β (high-temperature) phases of crystalline CH_3SH either involve cooling from the liquid phase or they lack sufficient details for independent duplication. We found that the α phase formed slowly on warming amorphous CH_3SH, but that a two-step process gave the same solid faster. First, CH_3SH was rapidly condensed onto a 70 K substrate so as to give an increase in the resulting ice's thickness of ∼15 μm hour^{-1}. Next, the sample was warmed to 100 K over about 10 minutes. This procedure quickly and reliably produced the pure α crystalline phase of CH_3SH.

Of the three CH_3SH solids we studied, the β phase was the most challenging to make in a pure form. The transition between α- and β-crystalline CH_3SH occurs[5] at 137.6 K, well above the temperature at which our samples sublimed. Therefore, it was impossible to warm either an amorphous or an α-crystalline sample to form the β phase or to deposit CH_3SH at 137.6 K to give the β phase directly. To produce this high-temperature phase we deposited CH_3SH at 110 K at a rate that gave a change in ice thickness of ∼1 μm hour^{-1}. The combination of the substrate's temperature and the energy released by CH_3SH condensation was sufficient to produce the pure β phase which then, in agreement with previous reports, was easily studied at lower temperatures without fear of a rapid β → α conversion.

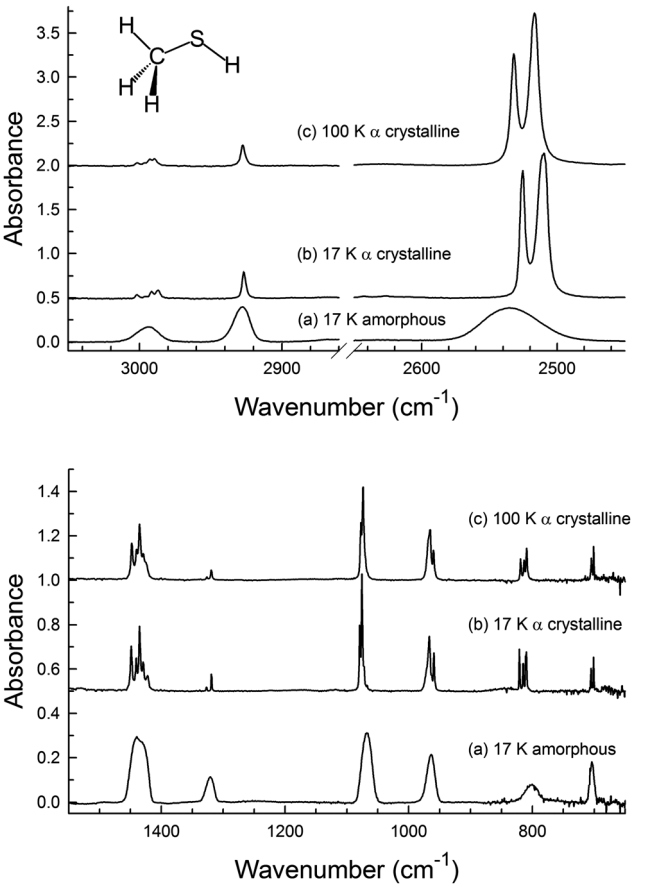

Fig. 2 Infrared spectra of amorphous CH_3SH at 17 K compared to the same regions for α-crystalline CH_3SH at 17 and 100 K. The thickness of the amorphous ice was about 7 μm, whereas the thickness of the crystalline sample was about 3 μm. Spectra are offset vertically for clarity. Note the different vertical scales of the two panels.

Fig. 2 and 3 show mid-IR spectra of the amorphous and crystalline forms of CH_3SH prepared as just described. These spectra show positions and intensities of the various IR features and permit quick comparisons. The amorphous phase's spectrum, seen at the bottom of Fig. 2, displays the rounded features already mentioned, whereas spectra of the α (Fig. 2) and β (Fig. 3) forms of CH_3SH possess the splittings and shifts more characteristic of crystalline solids. Tables 1 and 2 give positions of the more-prominent peaks of these spectra.

Of all the IR features of CH_3SH, of greatest interest to us was the intense S–H stretching mode (ν_3, 2535 cm^{-1}) in amorphous CH_3SH. Its position and strength suggest that it is this absorbance that is most likely to yield astronomical applications, our original motivation. Fig. 4 shows how this feature changed as an amorphous CH_3SH ice was warmed slowly. Between 17 and 60 K,

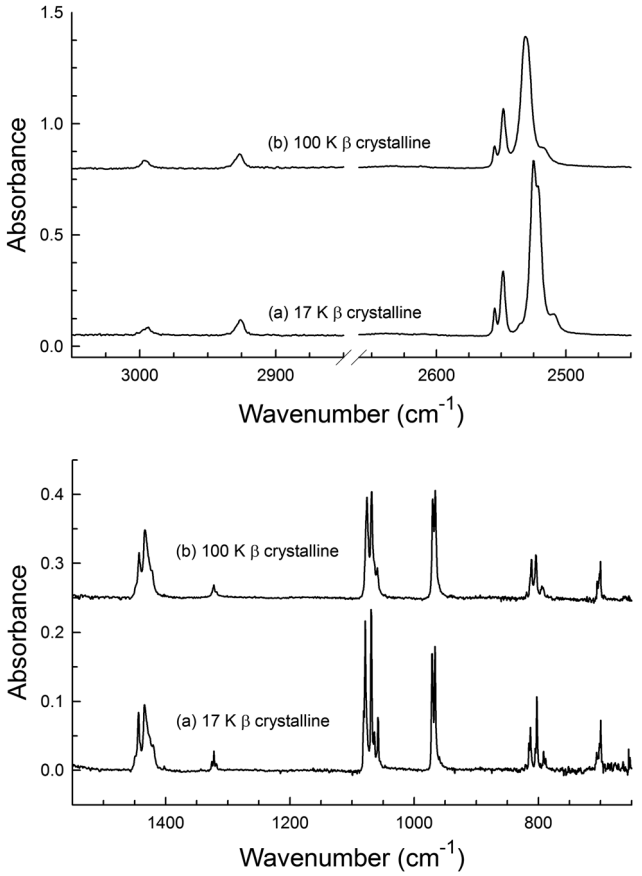

Fig. 3 Infrared spectra of β-crystalline CH_3SH at 17 and 100 K. The thickness of the sample was about 3 μm. Spectra are offset vertically for clarity. Note the different vertical scales of the two panels.

few changes were observed, but after additional warming to 65 K, and holding there overnight (~15 hours), changes in shape were seen that indicated the formation of the β (high temperature) crystalline phase or perhaps a solid that was a combination of more than one form of CH_3SH. Subsequent warming to 85 K sharpened all IR peaks considerably, and on sitting at 90 K the spectrum evolved into that of the pure α (low temperature) phase. Additional warming resulted in complete sublimation of the sample near 120 K in a minute or less. All such changes were irreversible.

In addition to measuring IR peak positions, we also measured IR intensities for all but one of the fundamental vibrations of amorphous CH_3SH at 17 K and for four fundamentals of the crystalline phases at 17 and 100 K. This was done by recording IR spectra of ices at multiple thicknesses, integrating individual absorbances in each spectrum, and graphing the values of such areas as a function of ice thickness (h). Such plots had correlation coefficients of 0.98 or better, with most above 0.99, showing that the IR features studied were not saturated. The slope of each such line was the quantity in parentheses in eqn (3), from which apparent band strength (A') was calculated.

$$\int_{\text{band}} (\text{Absorbance}) \mathrm{d}\tilde{\nu} = \left(\frac{\rho_N A'}{2.303}\right) h \qquad (3)$$

In this equation, ρ_N is the ice sample's number density, here as molecules cm^{-3}, to which we return in our Discussion. See our recent papers[32,33] and the much earlier work of Hollenberg and Dows[34] for details.

Table 2 gives band strengths A' for the main features of amorphous CH_3SH, along with the integration ranges used, whereas Table 3 gives A' values for four vibrations of α and β CH_3SH. For these two crystalline phases, values are given for both 17 and 100 K. For the difference, usually small, between apparent band strength A' and absolute band strength A, see Hudson *et al.*[32,33] Those two papers, and our more-recent one[35] contain estimates of ~1% for the uncertainty in A' for stronger bands (*e.g.*, ν_3 and ν_6), rising to as much as 5% for the weaker ones (*e.g.*, ν_5 and ν_8).

An immediate application of our A' values, and something of a check on them, came from measuring the vapor pressures of the α and β forms of CH_3SH at 110 K using the method of Khanna *et al.*[36] Combining Khanna's eqn (3), and our own eqn (3) above, gives

$$\int_{\text{band}} (\text{Absorbance}) \mathrm{d}\tilde{\nu} = \left(\frac{FA'}{2.303}\right) t \qquad (4)$$

where F is the flux of CH_3SH molecules escaping the substrate, at 110 K in our case, at time t. A graph of the area of an IR band, the left-hand side of (4), at successive times gave a straight line with slope = ($F{\cdot}A'/2.303$) from which F could be determined since A' already had been measured (Table 3). Substituting F into the standard kinetic theory relation

$$p = F\sqrt{2\pi mkT} \qquad (5)$$

then gave a vapor pressure p at 110 K, with m being the mass of a CH_3SH molecule. Measurements with the IR features listed in Table 3 gave 4.3×10^{-7} torr ($\pm 0.4 \times 10^{-7}$ torr) for α CH_3SH and 6.8×10^{-7} torr ($\pm 0.5 \times 10^{-7}$ torr) for β CH_3CH. Extrapolations of the data[5] on liquid CH_3SH give 5.2×10^{-7} torr, so that we take our results as reasonable.

Attempts to measure the rates of interconversion between the crystalline forms of CH_3SH met with little success. Conversions of the pure lower-temperature phase of CH_3SH into the high-temperature phase (α → β) were exceptionally slow, with only meager evidence for any conversion after about 24 hours at 100 K. No clear indications were obtained for the reverse conversion (β → α) at 110 K, and none were expected given the experience near 140 K of others.[12]

In addition to the IR bands listed in Tables 1 and 2, all assigned to fundamental vibrations of CH_3SH, numerous other small peaks were observed in the IR spectrum of methanethiol. Their study is left to the future, along with explorations of band strengths of near- and far-IR features.

4. Discussion

4.1 Refractive indices and densities

Number densities (ρ_N) were needed to use eqn (3) to compute the CH_3SH infrared band strengths of Tables 2 and 3, but few

Table 1 Positions of some IR features of crystalline CH_3SH at 17 and 100 K[a]

		α-Crystalline		β-Crystalline	
Vibration	Approx. description	17 K	100 K	17 K	100 K
ν_1, ν_9	$-CH_3$ antisymm stretch	3001.6 2991.5 2987.0	3001.8 2992.8 2989.7	2994.0	2996.2
ν_2	$-CH_3$ symm stretch	2926.7	2927.4	2925.8	2926.6
ν_3	SH stretch	2525.6 2510.5	2532.0 2516.9	2555.0 2548.7 2525.1 2509.2	2555.2 2548.5 2531.4 2516.8
ν_4, ν_{10}	$-CH_3$ antisymm def	1448.7 1440.7 1435.3 1429.5 1422.2	1448.0 1440.1 1435.4 1429.3 1425.6 u sh	1448.8 1443.8 1434.0	1448.0 1443.0 1434.2
ν_5	$-CH_3$ symm def	1327.1 1319.1	1326.5 1319.4	1325.6 1322.5 1318.4	1326.1 u sh 1322.6 1319.1
ν_6	$-CH_3$ rock	1079.2 1075.6 1072.6 u sh	1077.5 1073.9 1070.7	1078.9 1075.8 1069.2 1058.0	1076.4 1074.2 1068.7 1059.4
ν_{11}	$-CH_3$ rock	966.8 959.2	965.5 959.9	971.2 966.4	970.2 966.2
ν_7	C–S–H bend	821.0 815.0 810.0	819.1 813.5 809.4	821.2 815.3 812.9 802.5	819.0 813.2 811.1 803.9
ν_8	C–S stretch	705.1 701.0	704.8 700.9	706.3 701.9 699.6	705.5 700.0

[a] Positions are in cm^{-1}; vibrational assignments as suggested by May and Pace;[11] u sh = unresolved shoulder.

Table 2 Positions of some IR features of amorphous CH_3SH at 17 K[a]

Vibration	Approx. description	Position/cm^{-1}	$A'/10^{-18}$ cm molecule^{-1}	Integration range/cm^{-1}
ν_1, ν_9	$-CH_3$ antisymm stretch	2992.9	0.913	3020–2960
ν_2	$-CH_3$ symm stretch	2927.8	1.62	2960–2900
ν_3	SH stretch	2534.8	5.41	2600–2450
ν_4, ν_{10}	$-CH_3$ antisymm def	1438.2	2.45	1470–1400
ν_5	$-CH_3$ symm def	1320.1	0.444	1340–1300
ν_6	$-CH_3$ rock	1066.9	1.76	1100–1030
ν_{11}	$-CH_3$ rock	963.2	0.999	1000–930
ν_7	C–S–H bend	800.5	0.510	840–750
ν_8	C–S stretch	703.3	0.418	720–685

[a] Vibrational assignments and descriptions as suggested by May and Pace.[11]

values of ρ_N for solid CH_3SH are found in the literature. To calculate ρ_N for amorphous CH_3SH, we combined our data with eqn (6) below, the simplest form of the Lorentz–Lorenz relation. In this equation, N_A is Avogadro's number (molecules mol^{-1}), α_{CH_3SH} is the polarizability of CH_3SH (cm^3 $molecule^{-1}$), M is the molar mass of CH_3SH (48.107 g mol^{-1}), ρ is density (g cm^{-3}), and n is taken from our measurements.

$$(4\pi/3)N_A\alpha_{CH_3SH} = (M/\rho)\,(n^2 - 1)/(n^2 + 2) \quad (6)$$

Using $\alpha_{CH_3SH} = 5.40 \times 10^{-24}$ cm^3 $molecule^{-1}$ from Szmytkowski *et al.*,[37] our $n = 1.542$ for crystalline CH_3SH gives $\rho = 1.11$ g cm^{-3} in reasonable agreement with the 1.15 g cm^{-3} of May and Pace.[12] For amorphous CH_3SH and our $n = 1.417$, the same calculation gives $\rho = 0.888$ g cm^{-3} compared to 0.866 g cm^{-3} for liquid CH_3SH.[38] As expected, liquid CH_3SH and amorphous CH_3SH have similar densities. Our two values of ρ gave $\rho_N = 1.11 \times 10^{22}$ molecules cm^{-3} and $\rho_N = 1.39 \times 10^{22}$ molecules cm^{-3} for amorphous and crystalline CH_3SH, respectively.

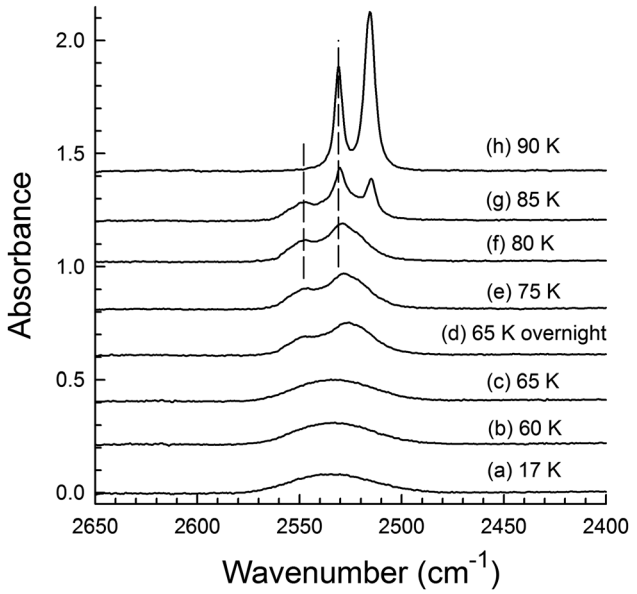

Fig. 4 Spectra recorded on warming amorphous CH_3SH from 17 to 90 K. The thickness of the sample was about 1.4 μm. Spectra are offset vertically for clarity. The dashed, vertical lines near the top indicate peak positions for the β-crystalline phase of CH_3SH. See the text.

Table 3 IR band strengths (A') for crystalline CH_3SH ices at 17 and 100 K[a]

	α-Crystalline		β-Crystalline	
Vibration	17 K	100 K	17 K	100 K
ν_2	0.614	0.570	0.529	0.451
ν_3	12.6	12.9	12.6	10.8
ν_6	1.32	1.37	1.68	1.70
ν_{11}	1.21	1.16	1.08	1.09

[a] Units of A' are 10^{-18} cm molecule^{-1}, as in Table 2; integration ranges were similar to those of Table 2.

4.2 Infrared spectra

An isolated methanethiol molecule possesses a plane of symmetry defined by the H–S–C–H sequence with the two hydrogens in a staggered conformation (Fig. 2).[11] With only this σ symmetry element, CH_3SH belongs to the C_s point group. The molecule's $3N - 6 = 3(6)–6 = 12$ fundamental vibrations belong to symmetry species $\Gamma_{red} = 8A' + 4A''$, each vibration being IR active. Since there are no degeneracies, twelve vibrational features should be observed. The ν_{12} vibration is a low-frequency torsional motion below[13] the region we studied, but we obtained evidence for the other eleven modes. Their assignments are in our Tables 1 and 2, and most can be made with reasonable confidence on the basis of gas-phase spectra. The main uncertainties are with two sets of features, the ν_1 and ν_9 absorbances that overlap around 2992 cm^{-1} and the ν_4 and ν_{10} peaks that do the same near 1436 cm^{-1}. The other seven vibrations show distinct peaks in the regions expected, with some peaks displaying considerable splitting for ices in the α- and β-crystalline phases. It should be kept in mind that mixing among these solid-phase modes occurs, so that the vibrational motions are not as simple as Tables 1 and 2 imply.

We already have mentioned ambiguities associated with some of the previous papers on the IR spectra of solid CH_3SH. Initially, the lack of some important details in earlier work hindered its direct comparison with the results presented here, but the main source of the discrepancies can now be traced to the first page of May and Pace.[12] Spectra of their low-temperature crystalline phase of CH_3SH were incorrectly identified there as those drawn with solid (unbroken) lines in the figures, but they should have been identified as traces drawn with dotted lines. Conversely, the spectra of the high-temperature phase should have been identified as those drawn with solid lines, not those with dotted lines. With these changes, the figures, text, and table of May and Pace[12] agree with one another, with earlier work,[11] with the later results of Wolff and Szydlowski,[13] and with the new results presented here. We also can now say that the unlabeled spectra of CH_3SH in Fig. 2 of May and Pace[12] are for, from top to bottom, the high-temperature crystalline phase (β), a mixture of the two crystalline phases (α + β), and the low-temperature (α), respectively.

Now confident in the connections between published CH_3SH spectra and our own, we can compare them. In general, our IR spectra of crystalline CH_3SH ices at 100 K closely resemble those of both May and Pace[12] and Wolff and Szydlowski.[13] The spectral resolution employed in these earlier papers was unspecified, but the band shapes resemble those in our spectra and peak positions agree within about 1–2 cm^{-1}. The lower trace of Fig. 3 in May and Pace[11] is the only published full spectrum we have found for solid CH_3SH. The size and quality of that figure, and especially its lack of a scale on the vertical axis, make a quantitative comparison impossible. Moreover, the sample's phase was not specifically stated. Qualitatively, however, it resembles our own spectra.

A new result of the present paper is spectra of CH_3SH under 80 K. Fig. 4 shows that amorphous CH_3SH exhibits little spectral variation on warming from 17 K until about 60 K. For the crystalline phases of CH_3SH, Fig. 1 and 2 show that the main changes on cooling from 100 to 17 K is that the IR features are sharper and more intense and shifted slightly. Table 3 gives band strengths for a few spectral features of each crystalline phase, from which it is apparent that the α and β forms have about the same intensities and that they vary little with temperature, as also indicated in Fig. 1 and 2. All spectral changes with crystalline ices between 17 and 100 K were reversible with temperature.

In Fig. 4 it is interesting that warming the amorphous CH_3SH sample to 80 K first produced an ice with IR peaks at 2548 and 2529 cm^{-1}, closer to the larger features of the higher-temperature (β) crystalline phase (2548, 2531 cm^{-1}) than those of the expected lower-temperature α phase (2532, 2517 cm^{-1}). In that same figure, the two dashed, vertical lines indicate the β phase's peaks. The intermediate solid observed at 65–85 K could be an annealed amorphous ice or perhaps an unreported metastable phase of CH_3SH, which evolved into the α-crystalline phase on further heating. However, when amorphous CH_3SH crystallizes it might also be that the β phase is kinetically favored, with further heating above 85 K giving the α phase

as the thermodynamically-favored solid. Support for this interpretation could come through Ostwald's step rule,[39] which predicts that the initially-formed phase on crystallization is the one that most resembles the starting material in structure.[39–41] Since an amorphous solid's structure can be considered as resembling that of a liquid, and liquid CH_3SH freezes into the β phase, then the suggestion that amorphous CH_3SH might also do so is not surprising. Although we lean toward this interpretation, we have no other firmly established and unequivocal example of this behavior among the many amorphous ices we have studied.

A final comparison is to CH_3OH, for which a careful study has been published by Gálvez *et al.*[7] Both CH_3OH and CH_3SH form amorphous ices by direct deposition from the gas phase, each possesses two crystalline phases, the conversions between the upper- and lower-temperature crystalline phases are slow, and for both compounds there is a question about the existence of a metastable solid phase. As with our discussion of CH_3SH, Gálvez *et al.* discount the possibility that a metastable form of CH_3OH is produced, albeit with a different line of argument than we have presented.[7] A review of previous work on CH_3OH ices in our laboratory finds no clear evidence for a metastable form.[42–44] New far-IR studies of both CH_3OH and CH_3SH could be interesting since spectra in that region can be very sensitive to phase.[43] Diffraction studies on CH_3SH ices also could be revealing.

The original motivation for this investigation was possible future applications to astrochemical problems, and so it is appropriate to end with that subject. Since dense interstellar clouds can have temperatures as low as 10 K, any solid CH_3SH within them is expected to exist either in the amorphous phase or dispersed in other icy materials. In either case the strongest IR feature is expected to be the molecule's ν_3 band near 2535 cm^{-1} (λ = 3.945 μm). As solid methanol has a weak absorption in that region, well-resolved, low-noise observations will be needed to distinguish CH_3SH from CH_3OH. Concerning Solar System objects, the IR reflection spectrum of Jupiter's moon Europa has a weak but distinct inflection at roughly the position of methanethiol's strong ν_3 feature.[45] Progress on astrochemical problems such as these will depend on future laboratory work, such as an evaluation of the influence of the presence of other ices, particularly frozen H_2O, on the spectral results we have presented. Quantitative comparisons to gas-phase reaction chemistry[46] and investigations into solid-phase chemistry will be facilitated by optical constants of CH_3SH in a variety of solids. The present work also should aid in the laboratory study of the other interstellar thiol, C_2H_5SH.[47]

5. Summary and conclusions

In this work, IR spectra of amorphous CH_3SH have been presented for the first time along with a full sequence of mid-IR spectra on warming. Evidence for a competition between kinetic and thermodynamic control during crystallization is described. Spectra of two crystalline phases are reported for the first time at a temperature below 77 K. Procedures are described for making three solid phases of CH_3SH by gas-phase deposition. Values of the refractive index of solid CH_3SH at two temperatures have been measured and used to calculate ice densities, which in turn have been combined with IR spectra to give apparent band strengths (A') and to estimate the vapor pressures at 110 K for α- and β-CH_3SH. Comparisons have been made to CH_3OH under similar conditions and some confusion in the literature concerning the IR spectra of solid CH_3SH phases has been removed.

Acknowledgements

Robert Ferrante digitized some literature spectra for comparison to the new work presented here. He and Perry Gerakines worked on the computer routine for fitting fringe patterns, a version of which is available at http://science.gsfc.nasa.gov/691/cosmicice/constants.html for interested parties. This investigation was supported by a grant from NASA's Astrophysics Research and Analysis program with additional funding from the NASA Astrobiology Institute's Goddard Center for Astrobiology.

Notes and references

1 R. A. Linke, M. A. Frerking and P. Thaddeus, *Astrophys. J.*, 1979, **234**, L139.
2 C. B. Pilcher, *Astrobiology*, 2003, **3**, 471.
3 S. Vance, L. E. Christensen, C. R. Webster and K. Sung, *Planet. Space Sci.*, 2011, **59**, 299.
4 S. D. Domagal-Goldman, V. S. Meadows and M. W. Claire, *Astrobiology*, 2011, **11**, 419.
5 H. Russell, D. W. Osborne and D. M. Yost, *J. Am. Chem. Soc.*, 1942, **64**, 165.
6 M. Falk and E. Whalley, *J. Chem. Phys.*, 1961, **34**, 1554.
7 Ó. Gálvez, B. Maté, B. Martín-Llorente, V. Herrero and R. Escribano, *J. Phys. Chem. A*, 2009, **113**, 3321.
8 T. Lin, C. Hsing, C. Wei and J. Kuo, *Phys. Chem. Chem. Phys.*, 2016, **18**, 2736.
9 E. L. Pace and L. J. Noe, *J. Chem. Phys.*, 1968, **49**, 5317.
10 E. D. Sprague, K. Takeda, J. T. Wang and F. Williams, *Can. J. Chem.*, 1974, **52**, 2840.
11 I. W. May and E. L. Pace, *Spectrochim. Acta*, 1968, **24A**, 1605.
12 I. W. May and E. L. Pace, *Spectrochim. Acta*, 1969, **25A**, 1903.
13 H. Wolff and J. Szydlowski, *THEOCHEM*, 1987, **160**, 221.
14 M. H. Moore, B. Donn and R. L. Hudson, *Icarus*, 1988, **74**, 399.
15 M. H. Moore, R. L. Hudson and R. W. Carlson, *Icarus*, 2007, **189**, 409.
16 M. Loeffler and R. L. Hudson, *Geophys. Res. Lett.*, 2010, **37**, 19201.
17 M. Loeffler and R. L. Hudson, *Icarus*, 2012, **219**, 561.
18 M. J. Loeffler, R. L. Hudson, N. J. Chanover and A. A. Simon, *Icarus*, 2015, **258**, 181.
19 M. J. Loeffler, R. L. Hudson, N. J. Chanover and A. A. Simon, *Icarus*, 2016, **271**, 265.

20 M. H. Moore, R. F. Ferrante, W. J. Moore and R. L. Hudson, *Astrophys. J., Suppl. Ser.*, 2010, **191**, 96.
21 K. E. Tempelmeyer and D. W. Mills, *J. Appl. Phys.*, 1968, **39**, 2968.
22 C. Romanescu, J. Marschall, D. Kim, A. Khatiwada and K. S. Kalogerakis, *Icarus*, 2010, **205**, 695.
23 D. M. Byler and W. V. Gerasimowicz, *THEOCHEM*, 1984, **112**, 207.
24 J. Sun, S. Hu, K. R. Sharma, B. Ni and Z. Yuan, *Water Res.*, 2015, **69**, 80.
25 H. Yamada and W. Person, *J. Chem. Phys.*, 1963, **38**, 1253.
26 H. Yamada and W. Person, *J. Chem. Phys.*, 1964a, **40**, 309.
27 H. Yamada and W. Person, *J. Chem. Phys.*, 1964b, **41**, 2478.
28 M. Á. Satorre, M. Domingo, C. Millán, R. Luna, R. Vilaplana and C. Santonja, *Planet. Space Sci.*, 2008, **56**, 1748.
29 C. W. Garland, J. W. Nibler and D. P. Shoemaker, *Experiments in Physical Chemistry*, McGraw Hill, New York, 2003, p. 53.
30 O. S. Heavens, *Optical Properties of Thin Solid Films*, Dover, New York, 2nd edn, 2011, p. 114, (Original printing: 1955, Butterworths Scientific Publ. London).
31 B. H. Torrie, O. S. Binbrek, M. Strauss and I. P. Swainson, *J. Solid State Chem.*, 2002, **166**, 415.
32 R. L. Hudson, R. F. Ferrante and M. H. Moore, *Icarus*, 2014, **228**, 276.
33 R. L. Hudson, P. A. Gerakines and M. H. Moore, *Icarus*, 2014, **243**, 148.
34 J. Hollenberg and D. A. Dows, *J. Chem. Phys.*, 1961, **34**, 1061.
35 R. L. Hudson, P. A. Gerakines and M. J. Loeffler, *Phys. Chem. Chem. Phys.*, 2015, **17**, 12545.
36 R. K. Khanna, J. E. Allen Jr, C. M. Masterson and G. Zhao, *J. Phys. Chem.*, 1990, **94**, 440.
37 C. Szmytkowski, G. Kasperski and P. Moiejko, *J. Phys. B: At., Mol. Opt. Phys.*, 1995, **28**, L629.
38 R. C. Weast, *Handbook of Chemistry and Physics*, 61st edn, 1980, p. C-412.
39 W. Ostwald, *Z. Phys. Chem.*, 1897, **22**, 289.
40 T. Threlfall, *Org. Process Res. Dev.*, 2003, **7**, 1017.
41 S. Chung, Y. Kim, J. Kim and Y. Kim, *Nat. Phys.*, 2009, **5**, 68.
42 R. L. Hudson and M. H. Moore, *Icarus*, 2000, **145**, 661.
43 R. L. Hudson and M. H. Moore, *Radiat. Phys. Chem.*, 1995, **45**, 779.
44 M. H. Moore, R. F. Ferrante and J. A. Nuth III, *Planet. Space Sci.*, 1996, **44**, 927.
45 R. W. Carlson, W. M. Calvin, J. B. Dalton, G. B. Hansen, R. L. Hudson, R. E. Johnson, T. M. McCord and M. H. Moore, "Europa's Surface Composition", in *Europa*, ed. R. T. Pappalardo, W. B. McKinnon and K. Khurana, University of Arizona Press, Tucson, 2009, pp. 283–327.
46 N. Balucani, F. Leonori, R. Petrucci, P. Casavecchia, D. Skouteris and M. Rosi, *Mem. Soc. Astron. Ital. Suppl.*, 2011, **16**, 91.
47 L. Kolesniková, B. Tercero, J. Cernicharo, J. L. Alonso, A. M. Daly, B. P. Gordon and S. T. Shipman, *Astrophys. J.*, 2014, **748**, 1.